Energy dispatch schedule optimization and cost benefit analysis for grid-connected, photovoltaic-battery storage systems

A. Nottrott, J. Kleissl*, B. Washom

University of California, San Diego
Department of Mechanical and Aerospace Engineering
9500 Gilman Dr – EBU2
La Jolla, CA 92093-0411

*Corresponding Author:
Email: jkleissl@ucsd.edu
Tel.: (858) 534-8087
Fax: (858) 534-7599

Abstract

A linear programming (LP) routine was implemented to model optimal energy storage dispatch schedules for peak net load management and demand charge minimization in a grid-connected, combined photovoltaic-battery storage system (PV+ system). The LP leverages PV power output and load forecasts to minimize peak loads subject to elementary dynamical and electrical constraints of the PV+ system. Battery charge/discharge were simulated over a range of two PV+ system parameters (battery storage capacity and peak load reduction target) to obtain energy cost for a time-of-use pricing schedule and the net present value (NPV) of the battery storage system. The financial benefits of our optimized energy dispatch schedule were compared with basic off-peak charging/on-peak discharging and real-time load response dispatch strategies that did not use any forecast information. The NPV of the battery array increased significantly when the battery was operated on the optimized schedule compared to the off-peak/on-peak and real time dispatch schedules. These trends were attributed to increased battery lifetime and reduced demand charges attained under the optimized dispatch strategy. Our results show that Lithium-ion batteries can be a financially viable energy storage solution in demand side, energy cost management applications at an installed cost of about $400 - $500 per kWh (approximately 40-50% of 2011 market prices). The financial value of forecasting in energy storage dispatch optimization was calculated as a function of battery capacity ratio.

Keywords – Economics, Energy storage, Forecasting, Optimal scheduling, Solar power generation

Nomenclature

A	annual energy bill savings
E	energy
f	objective function
M	number of forecast update times
N	number of timesteps
NCC	number of charge cycles at 80% depth of discharge
NPV	net present value
OM	operation and maintenance costs
P	power (*dE/dt*)
R	power ramp rate (*dP/dt*)
r	discount rate
T	nominal battery lifetime
t	time.

Greek symbols

Δ	discrete change
ε	forecast accuracy (safety) factor.

Superscript

DC rating	DC nameplate rating of the PV array
m	forecast update index
max	maximum value
min	minimum value
n	time index
target	target value, objective
total	total energy capacity of the battery array.

Subscript

0	initial condition (*n = 0*)
l	load
lf	load forecast
o	PV+ output
opt	computed with LP optimization routine, i.e. Eqs. 1-3
p	PV output
pf	PV output forecast
s	battery (storage)
update	time between forecast updates.

Symbols

<> denotes a time average.

1. Introduction

Adoption of advanced energy storage technologies as a means to integrate renewable energy resources into electric grids will dramatically increase in the next decade. 28 states in the United States of America have enacted mandatory renewable portfolio standards (RPS) and 5 additional states have adopted voluntary RPSs. RPSs require electricity providers to obtain a minimum percentage of their power from renewable energy resources by a certain date [1]. The state of California has set an ambitious RPS of 33% renewable electricity generation by the year 2020 [2] and passed legislation to determine energy storage procurement targets for both privately and publicly owned utilities [3]. Although critical applications for large scale energy storage (and the associated costs, benefits and market potentials) have been clearly identified [4,5], dispatch strategies for stored energy that maximize the financial value of combined renewable generation and energy storage systems (hereafter RSS) are not well quantified or understood in an operational context [6].

Many models have been developed to determine optimal scheduling for stored energy dispatch in RSSs. The objectives of these modeling studies can be broadly classified in two categories, utility side applications and demand side applications [7]. Utility side applications focus on optimizing properties of the RSS output that are economically beneficial to electric utilities (e.g.

renewable capacity firming, transmission and distribution upgrade deferral, transmission support, etc.). The financial benefits associated with some utility side applications may be difficult to quantify (e.g. transmission support).

Demand side applications optimize the economics of the RSS when the system is installed "behind the meter". In this case economic benefits are usually quantified in terms of energy bill savings for the RSS owner who purchases power from an electric utility (e.g. time-of-use energy cost management, demand charge management, etc.). Lee & Chen [8] used an advanced multi-pass dynamic programming (AMPDP) algorithm to optimize contract capacities and optimal energy storage capacity of stand-alone BESSs for utility customers that incur time-of-use (TOU) electricity rates. They found that optimal BESS capacity could be determined and varied significantly based on the customer's load profile. A number of studies have investigated optimal energy storage capacity and dispatch, and economics for PV+ systems[1]. Su et al [9] implemented a closed-loop control system to modulate power output from a PV+ system for demand charge management, TOU energy price arbitrage, emergency power supply and transmission support. Su et al concluded that the economic viability of PV+ systems is site specific and depends strongly on the end user load shape, utility rate schedule, PV+ capacity and choice of application, however, their evaluation only considered a single PV+ system with fixed PV nameplate rating and battery capacity. Hoff et al [10] studied the economic benefits of PV+ for emergency power supply and demand charge management applications for typical industrial customers. Hoff et al found that financial benefits from emergency power supply exceeded benefits from demand charge management; however, they assumed that the entire battery capacity would be devoted to one application and only considered two PV+ systems with fixed PV nameplate rating and battery capacity. Shimada & Kurokawa [11] modeled annual energy bill savings for a PV+ system over a range of battery capacities using an approximate insolation forecast and a load forecast to determine the amount of night time charging required to minimize the cost of energy purchased by the customer from the electric utility during the following day. Shimada & Kurokawa found that the value of the PV+ system was significantly increased by using day-ahead, hourly insolation and load forecasts to inform the energy storage dispatch scheduling algorithm and identified optimal battery capacities in terms of end user peak load. Ru et al [12] used a mixed integer linear programming (MILP) framework to determine optimal battery energy capacity (in the context of marginal energy cost) for a PV+ system and implemented a peak reduction objective assuming perfect net load forecasts. The most comprehensive model to quantify the economic value of general RSS in demand side applications is the Distributed Energy Resources Customer Adoption Model [13]. DER-CAM minimizes costs of operating on-site customer generation considering combinations of many different distributed generation technologies, dispatched in a variety of demand side applications, and electrical tariffs.[2] Stadler et al [14] used DER-CAM to study demand charge management and CO_2 emissions minimization strategies in PV+ systems. Their results showed that for demand charge management it is most economically efficient to charge batteries from the

[1] The term PV+ was coined by Hoff et al [10] and refers to combined photovoltaic and battery energy storage systems where the battery is placed "behind the meter".

[2] The primary disadvantage of DER-CAM is that, due to its complexity and native software, the model is not yet suitable for widespread public release, although some DER-CAM functionality has been made available to end users through the Storage Viability and Optimization Web Service [15].

electric grid during off-peak hours, while charging batteries directly from zero emissions PV generation for CO_2 minimization results in extraordinarily high energy costs to the customer.

In this paper we consider an idealized PV+ system in which a PV array and a Lithium-ion battery array are connected to the utility electric grid (Fig. 1). The goal is to determine the optimal dispatch schedule for the energy stored in the battery to achieve a preset amount of load peak shaving (i.e. demand charge management). The optimization algorithm is formulated as a linear program (LP) and leverages day-ahead PV power output and load forecasts with regular updates to determine the best time to charge or discharge the battery subject to basic dynamical and electrical performance constraints of the PV+ system. System economics were quantified by the net present value (NPV) of the battery, and the financial value of PV power output and load forecasts in an energy bill reduction application of the PV+ system was calculated. We also computed the market price at which large scale (240 - 1270 kWh), Lithium-ion battery energy storage becomes financially viable in demand side, energy bill minimization applications. The model formulation and structure are described in Section 2, results from analysis of model output are presented in Section 3. Sections 4 and 5 are a discussion of our results and conclusions.

2. Methodology

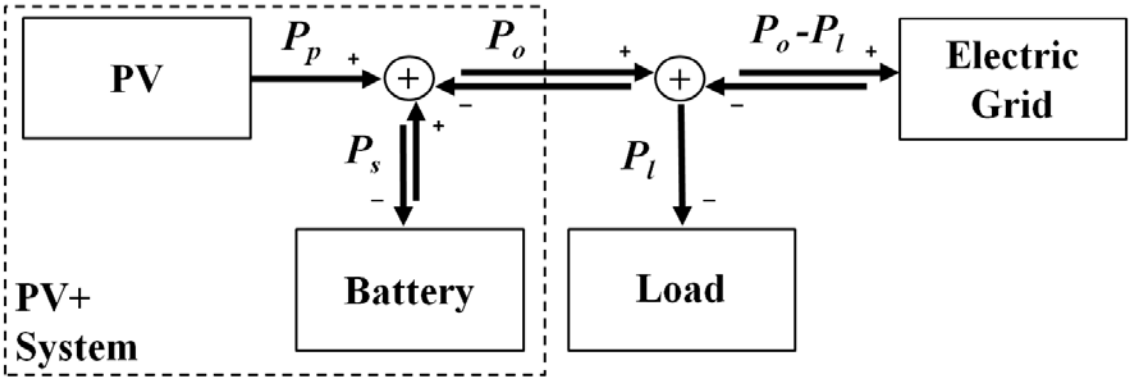

Figure 1 – A schematic of the system model illustrating the important components and power flows; the PV+ system is delineated by the dashed line. Positive and negative symbols indicate sign conventions for active power flows. Because the inverter is assumed to be lossless it is not shown in this diagram. The battery management system is included in the battery, which allows "black box" treatment of complex electrical dynamics and transients within the battery.

2.1 Linear optimization model

Fig. 1 shows a schematic of the idealized PV+ system in which a PV array, a Lithium-ion battery array, and a load are connected to the utility electric grid. The PV array and battery array generate DC power which is converted to AC power via a lossless bidirectional inverter, and all power electronics (e.g. DC-DC converters and battery management systems) are assumed to be 100% efficient. The charging/discharging response of the battery is assumed to be practically instantaneous so that energy from the battery may be dispatched "on demand". This assumption is justified because the response time of Li-ion type batteries is O(ms) and energy dispatch from the battery was modeled on 15 min intervals. The battery is treated as a black box within the model, meaning that the charging and discharging efficiency of the battery does not depend on the charge/discharge power P_s, and P_s can take any values within the specified limits of the nominal battery performance. The utility customer's net load is given by P_o-P_l.

The model is formulated as a discrete-time, linear optimization problem (linear program; LP).

$$min\left\{f(P_{lf}^n, P_o^n) = \sum_{k=1}^{N} (P_{lf}^k - P_o^k)\Delta t \text{, while } P_{lf}^k > 0 \text{ and } P_{lf}^k > P_{pf}^k \right. \quad (1)$$

such that

$$P_{pf}^n + P_s^n = P_o^n \quad (2a)$$

$$\frac{E^{n+1} - E^n}{\Delta t} = P^n \quad (2b)$$

$$\frac{P^{n+1} - P^n}{\Delta t} = R^n \quad (2c)$$

$$E_s^{min} \leq \sum_{k=1}^{n} P_s^k \Delta t + E_0 \leq E_s^{max} \quad (3a)$$

$$P_s^{min} \leq P_s^n \leq P_s^{max} \quad (3b)$$

In Eqs. 1-3 E and P are energy and power. Variables with subscript *s* are related to the battery array, subscript *pf* refers to the PV power output forecast, subscript *lf* is the load forecast, subscript *o* denotes power flows to and from the PV+ system, and *0* indicates an initial condition. Integer superscript *n* is the current timestep, Δt is the timestep size and N denotes the maximum number of timesteps in the forecast horizon (e.g. N = 96 for a 24 h forecast horizon at 15 min sampling rate). Superscripts *min* and *max* indicate performance limits of the battery (i.e. maximum and minimum capacity or charging/disch arging rate). Eq. 1 minimizes net PV+ battery system power output (P_o) levels that fall below the forecast customer load (P_{lf}). In Eq. 1, *f* is a scalar valued objective function (or cost function) that corresponds to the energy shortage between the forecast customer load P_{lf} and the forecast PV power output P_{pf}. The condition $P_{lf}^n \geq 0$ ensures that battery charging and discharging is unrestricted during off-peak periods. The condition $P_{lf}^n > P_{pf}^n$ allows the battery to charge and discharge freely (i.e. there is no change in *f*) when the forecasted PV power output meets or exceeds the forecasted load. No cost is associated with selling or purchasing power from the electric grid in the LP, i.e. the model does not explicitly optimize on price arbitrage between the on-peak and off-peak energy markets. Price arbitrage is considered indirectly by forcing a reduction of on-peak demand and charging off-peak. Eqs. 2a,b are energy conservation (Kirchhoff's Law) and system dynamic respectively. Eqs. 2a,b are enforced as equality constraints in the LP. Eq. 3a requires that the energy stored in the battery is bounded within the capacity of the battery. Eq. 3b constrains the battery charging and discharging rate within the specified limits of the battery performance. Eqs. 3a,b are modeled as inequality constraints. The discrete-time, LP system is solved in MATLAB.

2.2 Time advancement and response to forecast errors

Fig. 2 shows the high level structure of the optimization algorithm. PV+ system parameters and day-ahead PV power output and load forecasts are inputs to the model (see Section 2.4). The application of the optimization algorithm depends on two conditional tests (top right in Fig. 2). Empirical testing of the model revealed that the optimization strategy performed poorly when $E_l < (E_s^{max} - E_s^{min})$ due to sub-optimal convergence of Eq. 1 in the LP optimization. Therefore, each day at midnight the 24-hour ahead forecast is used to determine if the useable capacity of the battery is large enough to supply the entire peak energy demand. The LP optimization is only conducted if the usable energy capacity of the battery is less than the energy capacity of the net load times a forecast accuracy factor ε (here ε = 0.85). ε is a safety factor which compensates for effects of systematic forecast bias. If the LP optimization is not conducted, the energy stored in

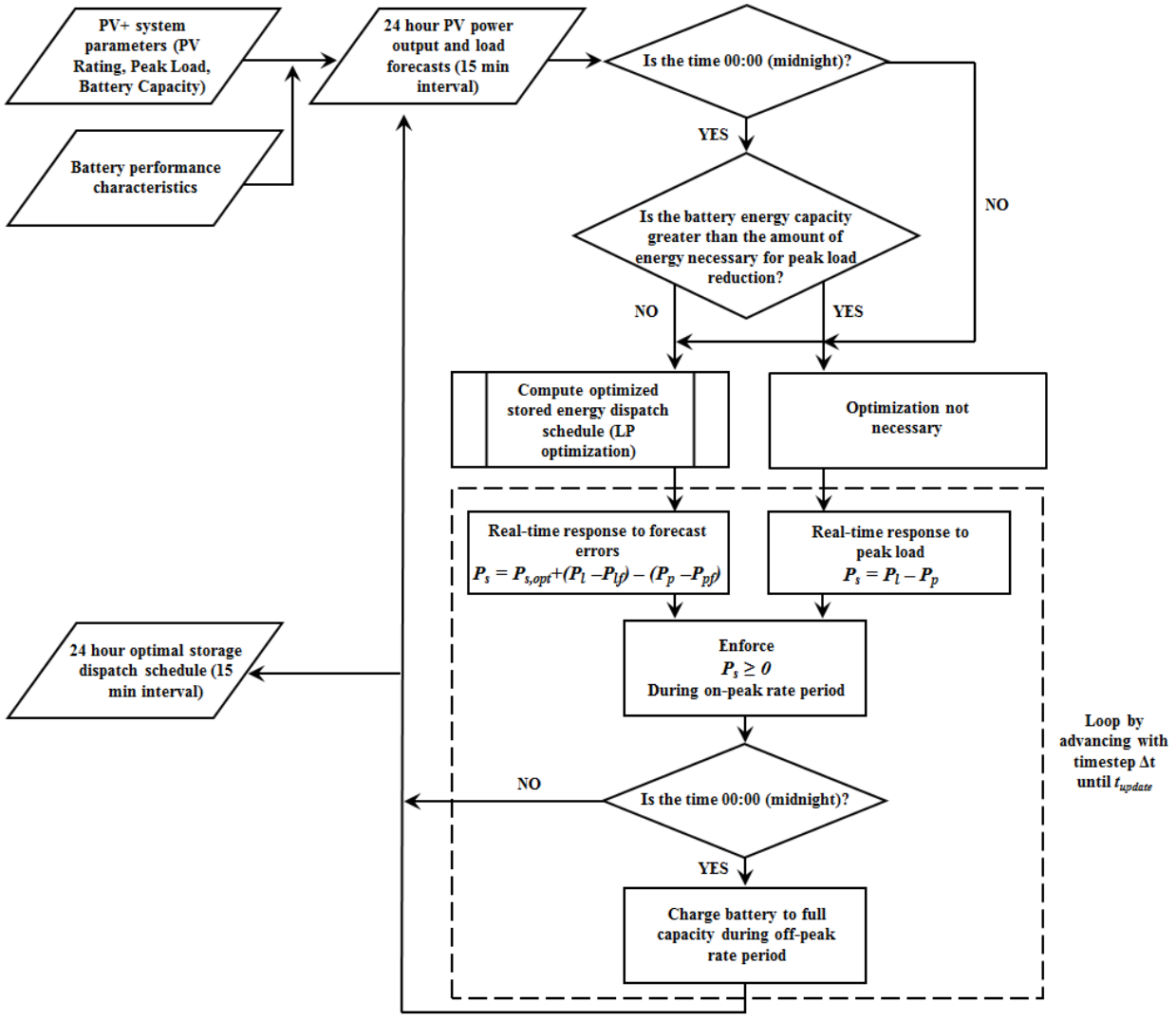

Figure 2 – Flowchart illustrating the important inputs, outputs and model processing steps in the dispatch schedule optimization algorithm.

the battery is dispatched in real-time to meet the net load. At each forecast update time the model output is an optimal, 24-hour ahead energy dispatch schedule (P_o) for the PV+ system.

PV power output forecasts (P_{pf}) and load forecasts (P_{lf}) are available for a finite time horizon $N \cdot \Delta t$ and are continuously updated on an interval t_{update}. The forecast horizon is $N \cdot \Delta t$ = 24 hours and Δt = 15 min. This type of information about future system output motivates a receding horizon approach for time advancement within the model. Initially an optimization is performed to compute the best dispatch schedule for the energy stored in the battery $\{P_s^n\}_{m=0}$ using all available information about the initial state of the system and PV power output and load forecasts until $N \cdot \Delta t$. Forecast updates are denoted by the integer subscript $m \in \mathbf{Z} = [0,M]$. The model is initialized at $n = 1$, $m = 0$ by requiring that $\{E_0\}_0$ has an arbitrary but fixed value (Eq. 3a), and allowing $\{P_s^1\}_0$ to take any value between P_s^{min} and P_s^{max} determined by the solution to Eq. 1. The optimization is conducted over $N \cdot \Delta t$ and the PV+ system operates according to the computed dispatch schedule until t_{update} when a new forecast is available. At that point the

optimization is repeated using new, 24 hour ahead PV output and load forecast data, and additional equality constraints are imposed in the LP to ensure that $\{P_s^{\,1}\}_{\mathrm{m}}$ in the current optimization is equal to $\{P_s^{\,n\_update}\}_{m-1}$ from the previous optimization (i.e. continuity of the storage dispatch schedule P_s is required between forecast updates).

$$\{P_s^1\}_m = \left\{P_s^{n_{update}}\right\}_{m-1} \tag{4}$$

The initial energy storage for the m^{th} iteration is set to,

$$\{E_0\}_m = \left\{E_0^{n_{update}-1}\right\}_{m-1}. \tag{5}$$

The system operates on the updated schedule for $n_{update} = t_{update}/\Delta t$ timesteps until a new forecast is obtained. This procedure is repeated to generate a continuous, optimal energy dispatch schedule for the battery.

The assumption of practically instantaneous battery response (see Section 2.1) permits incorporation of real time PV output and load data to improve the PV+ system performance during the forecast update interval t_{update}. Refinements are made to the optimal, 24-hour ahead schedule at each time increment between $n = 1$ and $n = n_{update}$ in order to compensate for errors in the PV output and load forecasts (dashed box in Fig. 2). At the forecast issue time ($n = 1$) the optimal stored energy dispatch schedule is computed over the entire 24 hour forecast horizon according to Eqs. 1-3 using only forecast information and the current state of the battery. The actual PV output and load are monitored in real time and the battery can respond to compensate for forecast errors. During off-peak rate periods this approach does not contribute to demand charge reduction, but it amounts to a renewables capacity firming application of the battery, i.e. the battery responds both to shortages and surpluses. During on-peak rate periods $P_S \geq 0$ is enforced, so the battery only responds to shortages. After a period t_{update} new forecast information is available and the optimal dispatch schedule is recalculated over the new forecast horizon. Conceptually one can interpret this procedure as a continuous perturbation to the optimal solution that arises due to forecast errors. At each forecast issue time the charge and output states of the battery are perturbed by a small amount from their expected states under the optimized solution due to the action of real time compensation for forecast errors.

2.3 PV+ system cost-benefit analysis

There are three PV+ system parameters in our model: PV array DC nameplate rating ($P_p^{\,DC\ rating}$), energy storage capacity ($E_s^{\,total}$) and the peak load reduction target ($P_l^{\,target}$). $P_l^{\,target}$ was chosen as a PV+ system parameter because the optimization algorithm targets demand charge management, and $P_l^{\,target}$ is linearly proportional to the customer's demand charge (see Appendix A). A more common choice to quantify the load capacity being managed by the PV+ system is battery capacity ratio, which is the quotient of the total energy storage capacity and the average daily load energy capacity ($E_s^{\,total}/\langle E_l \rangle$; [11]). It will be shown later (Section 3.4, Fig. 8a) that $P_l^{\,target}$ and $E_s^{\,total}/\langle E_l \rangle$ are consistent and both are valid PV+ system parameters. To evaluate feasible PV+ system designs a cost analysis was performed to determine the NPV of the battery storage system by calculating energy bill savings attained over the lifetime of the battery relative to capital costs of the storage system, annual operation and maintenance (O&M) costs and the discount rate. The net present value is estimated from

$$NPV = \sum_{t=0}^{T} \frac{A - OM}{(1+r)^t}, \tag{6}$$

where A is the value of annual energy bill savings extrapolated from 2009 data, OM is the annual O&M cost for operating the storage system (including energy costs for active cooling of the

battery array), *r* is the discount rate, *t* is the current year and *T* is the total lifetime of the battery in years. For *t = 0, OM* is equal to the capital costs incurred on the purchase and installation of the storage array and *A = 0*. In this study we assumed that annual O&M costs were constant and equal to 3% of the capital cost of storage. Annual energy bill savings are attributed solely to the use of energy storage in the PV+ system, and energy bill savings are assessed in terms of the difference between the annual energy costs with and without the application of battery energy storage. Electric utilities assess TOU energy pricing and demand charges for industrial customers. The energy bill was calculated using the San Diego Gas & Electric (SDGE) AL-TOU rate schedule for industrial customers. The AL-TOU tariff includes basic service fees, on-peak and non-coincident demand charges and TOU energy pricing (Table A.1; [16]). Non-coincident demand charges (see Table A.1) are assessed monthly based on the utility customer's maximum load (15 min interval) during the current month, not considering the rate periods in Table 1. If the maximum load during the previous 11 months was greater than the maximum load in the current month, the non-coincident demand charge is computed from 50% of the maximum load during the previous 11 months. This rate structure incentivizes customers to gradually reduce their monthly peak load in order minimize the non-coincident demand charge portion of their energy bill.

	Summer, May 1 - Sep 30	**Winter, Oct 1 - Apr 30**
On-peak	11:00 - 18:00, Weekdays	17:00 - 20:00, Weekdays
Semi-peak	6:00 - 11:00, Weekdays	6:00 - 17:00, Weekdays
	18:00 - 22:00, Weekdays	20:00 - 22:00, Weekdays
Off-peak	22:00 - 6:00, Weekdays	22:00 - 6:00, Weekdays
	Plus Weekends & Holidays	Plus Weekends & Holidays

Table 1 – San Diego Gas and Electric (SDGE) seasonal time-of-use rate periods for industrial customers (Schedule AL-TOU). The actual prices associated with energy and demand charges are listed in Table A.1 in Appendix A.

In order to quantify the financial advantages of our optimization strategy we compared the optimized dispatch schedule (OPT) with two storage dispatch schedules that did not use any PV output or load forecast information, a simple off-peak/on-peak, charge/discharge schedule (OFFON) and a real-time dispatch scenario (RT). For the OFFON schedule the battery undergoes one full charge cycle at 80% depth of discharge (DoD) per day. Charging and discharging rates are constant over the off-peak and on-peak periods defined in Table 1. OFFON is often used in real applications because it is simple, guarantees reduction in net load during the on-peak rate period, and maximizes off-peak, on-peak energy arbitrage. For the RT schedule the battery is charged to full capacity during the off-peak rate periods in Table 1 and discharged to meet the customer's actual net-load in real time. RT is also simple and attractive because the battery is only used when it is needed for peak load reduction thus increasing battery lifetime.

2.4 Battery System

The energy storage device is a Sanyo DCB-102 Lithium-ion battery array. A single Sanyo DCB-102 has nominal energy storage capacity of 1.59 kWh and minimum lifetime rating of 3000 cycles at 80% DoD. The DCB-102 has a maximum charging power of P_s^{min} = -340 W and a maximum discharging power of P_s^{max} = 720 W. The capital cost of the battery array was assumed to be $1000/kWh including installation costs. The number of charge cycles at 80% DoD over a period of *N* timesteps was calculated from Eq. 7.

$$NCC = \frac{1}{2}\sum_{n=1}^{N}\left|\frac{E_s^n - E_s^{n-1}}{0.8E_s^{total}}\right|, \quad (7)$$

In Eq. 7 *NCC* is the number of charge cycles and E_s^{total} is the total energy capacity of the battery array. To avoid overcharging or overdrawing of the battery array the model parameters E_s^{min} and E_s^{max} are set to $0.2E_s^{total}$ and $0.99E_s^{total}$, respectively.

2.5 Solar and Load Data

One year (2009) of 15 min DC power output data from one inverter of the EBU2 building rooftop PV array on the University of California, San Diego campus was used as the basis for P_p and P_{pf} (Fig. 3a). The PV array has a DC nameplate rating of 7.5 kW DC and the data was scaled to approximate the output of a larger system with a rating of $P_p^{DC\ rating}$ = 500 kW DC; for 15 min averages the relative variability of the output for a 500 kW or 7.5 kW are essentially identical [17]. The load data were obtained from 2009 UCSD campus load profiles (Fig. 3b).

2.6 Solar and Load Forecasts

Real forecasts (e.g. from numerical weather prediction) often produce large errors that are weather and location dependent [18].To make our results more generalizable and focus on the performance of battery dispatch strategies, a PV "forecast" was generated from the measured data. The 15 min PV output was filtered using a 45 min moving average window to generate the solar forecast P_{pf}. During clear and overcast conditions P_p (the actual PV power output) and P_{pf} (the forecast PV output) are very close since P_p is smooth, but in partly cloudy conditions P_p fluctuates randomly about $<P_{pf}>$. Uncertainty in the load forecast was simulated by incorporating random, normally distributed fluctuations with a standard deviation of 5% of the magnitude of the load in Fig. 3b.

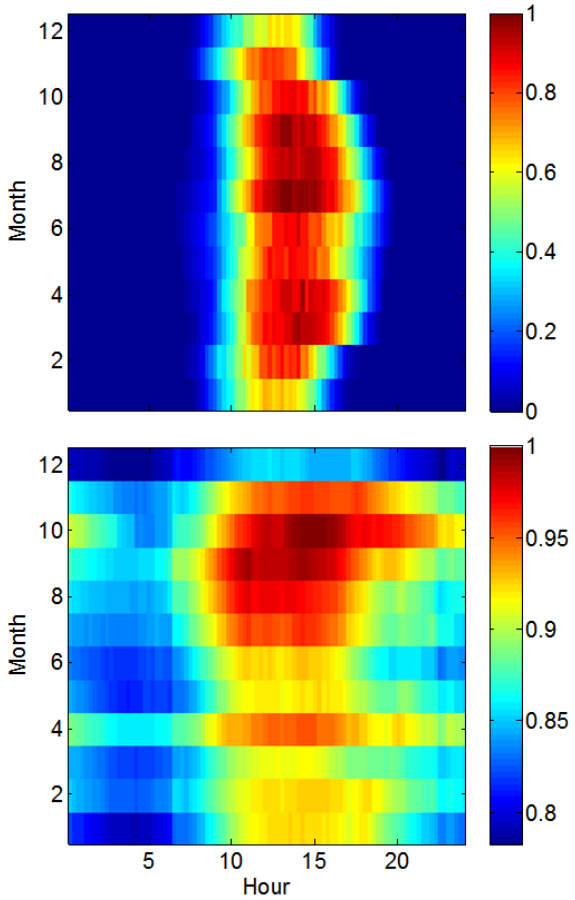

Figure 3 – Monthly climatologies (15 min resolution) of **a)** the measured PV array DC output normalized by the DC nameplate rating; **b)** the total measured load normalized by maximum annual demand (33.8 MW in October). The peak load profile is obtained by requiring that the maximum monthly peak load is $\{P_l^{max}\}_{monthly}$ - P_l^{target} and the excess "peak load" is the input to the optimization routine. Note that the peak in the PV array output usually occurs several hours earlier than the peak in the customer load.

3. Results

PV+ system performance was simulated for a wide range of peak load reduction targets (P_l^{target} = 240-1500 kW), battery storage capacities (E_s^{total} = 240-1270 kWh) and a PV array with a fixed nameplate rating of $P_p^{DC\ rating}$ = 500 kW DC in order to evaluate model performance and quantify the financial benefits that are realized when PV and load forecasts are applied to optimize the charge/discharge schedule of the battery. In total 602 cases were simulated for one year.

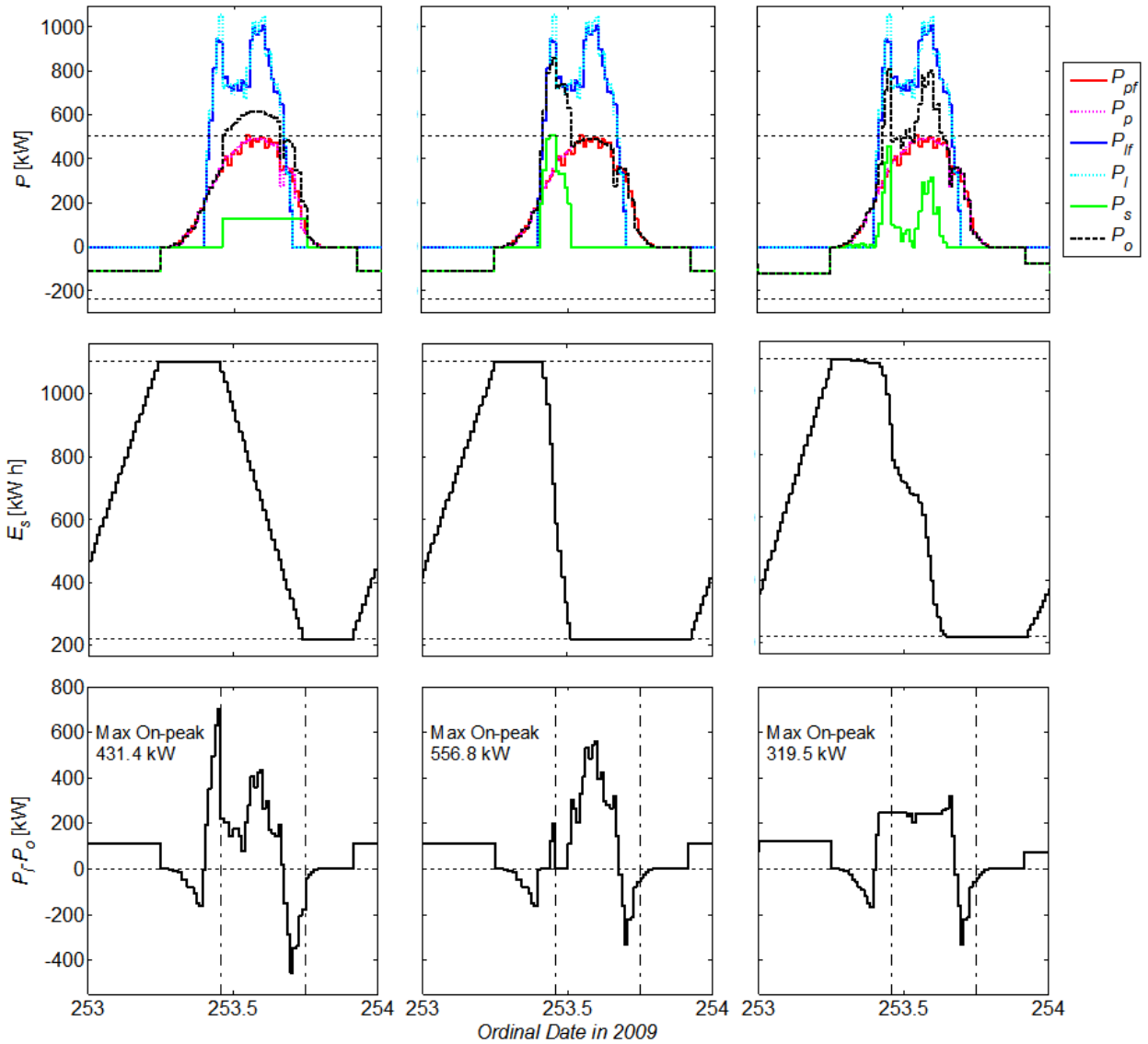

Figure 4 – Sample timeseries of model output data on September 9th, 2009 illustrating PV+ system power flows **(a,b,c)**, the battery charge state **(d,e,f)** and the net load on the electric grid **(g,h,i)**. Figs. 4a,d,g show model output when energy storage is dispatched according to the OFFON strategy, Figs. 4b,e,h show model output for the RT strategy and Figs. 4c,f,i show model output for the OPT strategy. Power flows in Figs. 4a,b,c are relative to the PV+ system so that $P_o > 0$ indicates net generation by the PV+ system and $P_o < 0$ indicates reverse power flow (i.e. the battery is charging from the grid). The fine dashed horizontal lines in Figs. 4a,b,c, indicate the maximum charging and discharging power of the battery array. The net load plotted in Figs. 4g,h,i is relative to the electric grid so that $(P_l - P_o) > 0$ indicates power flow from the grid to the customer and vice versa. The dash-dotted vertical line in Figs. 4g,h,i indicate the range of the on-peak period as defined in Table 1. The PV+ system parameters for the data shown in this figure are $P_p^{DC\ rating}$ = 500 kW, E_s^{total} = 1111 kWh and P_l^{target} = 1020 kW.

3.1 Time series of model output

Fig. 4 shows exemplary time series of model output data from September 9th, 2009 for P_l^{target} = 1020 kW and E_s^{total} = 1111 kWh. The columns in Fig. 4 show PV+ system power flows, battery charge state and net load on the electric grid for the OFFON, RT and OPT dispatch schedules. Figs. 4c,f,i illustrate superior performance of the optimized schedule over the OFFON and RT dispatch schedules that do not use PV output and load forecasts. For the given PV+ system

parameters the battery undergoes one complete charge cycle per day for all three dispatch schedules. Using the OFFON strategy the energy stored in the battery is dispatched concurrently

with the peak load, but the output power of the battery is too low during that time. Using the RT strategy the battery discharges too quickly leading to is complete discharge by the beginning of the on-peak rate period. With the OPT strategy the shape of the battery discharge curve closely approximates the shape of the peak load, and the net load during the on-peak rate period is relatively constant when compared with the off-peak/on-peak and real-time strategies (Fig. 4i).

Figs. 4g,h,i show that the maximum net load on the electric grid during the on-peak rate period (i.e. when higher demand charges are assessed by the utility) is smallest under the optimized schedule. For the data shown in Fig. 4 the optimization algorithm reduced the maximum on-peak, net load by 26% (112 kW) when compared with the OFFON schedule, and 43% (237 kW) when compared with the RT schedule. The small peak near the end of the on-peak rate period in Fig. 4i is due to under-forecasting of the net load resulting from an overestimation of the actual PV power output by the PV forecast and/or an underestimation of the peak load by the load forecast. This leads to the battery becoming discharged just before the end of the high load period.

3.2 Performance evaluation of the optimized dispatch schedule

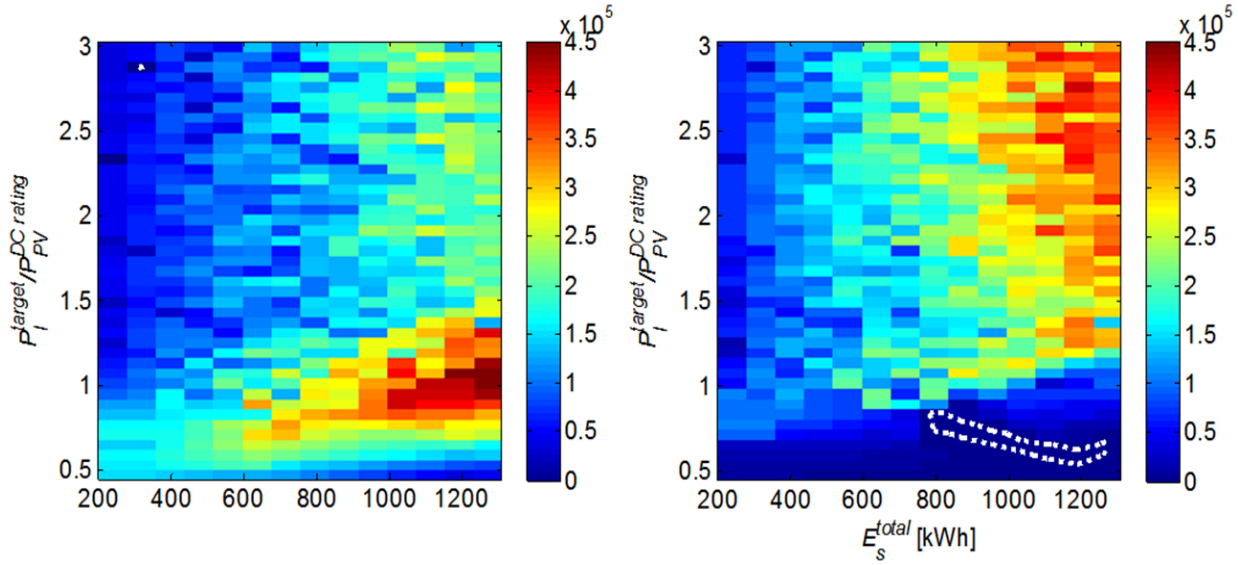

Figure 5 – Difference between the net present value (ΔNPV; Eq. 6) of the OPT schedule and **(a)** the OFFON schedule; **(b)** the RT schedule. The NPV difference for a broad range of battery capacities (E_s^{total}) and peak load reduction targets (P_l^{target}) are shown. The PV array nameplate rating was set to $P_p^{DC\ rating}$ = 500 kW DC. The units of the color scale are $USD and the dashed white line delineates the $0 contour.

Results from 2009 model output were extrapolated over the lifetime of the battery (3000 the charge cycles, Eq. 7) to estimate the NPV of the battery array. Fig. 5 shows the NPV gain of the OPT dispatch schedule over the OFFON (Fig. 5a) and RT (Fig. 5b) dispatch schedules for different battery capacities that were "tasked" with a broad range of peak load reduction targets (P_l^{target}). Total battery capacity (E_s^{total}) is plotted on the horizontal axis and the peak load

reduction target ratio ($P_l^{target}/P_p^{DC\ rating}$) is plotted on the vertical axis. Given that $P_p^{DC\ rating}$ is 500 kW, P_l^{target} ranges from 250 kW to 1500 kW). The color scale is the increase in NPV (ΔNPV) of the battery array in US dollars. Fig. 5 shows that operating the battery on the OPT dispatch schedule is more profitable than operating on the OFFON or RT schedules for most battery sizes and peak load capacities modeled in this study. The OPT strategy provides significantly more value than the OFFON strategy, especially in the range $E_s^{total} > 500$ kWh and $P_l^{target}/P_p^{DC\ rating} < 1.25$ where the NPV of the battery increases in the range \$150k-\$450k (or \$220/kWh of capacity) under the OPT scenario. When compared with the RT dispatch strategy, the OPT schedule increases the value of the battery array by about \$100k - \$400k (or \$270/kWh) for $E_s^{total} > 600$ kWh and $P_l^{target}/P_p^{DC\ rating} > 1.5$ (Fig. 5b). In Fig. 5a the increase in NPV becomes independent of P_l^{target} for large values of $P_l^{target}/P_p^{DC\ rating}$, because the demand charge savings are ultimately limited by the total battery capacity regardless of the dispatch schedule.

3.3 NPV of the battery array

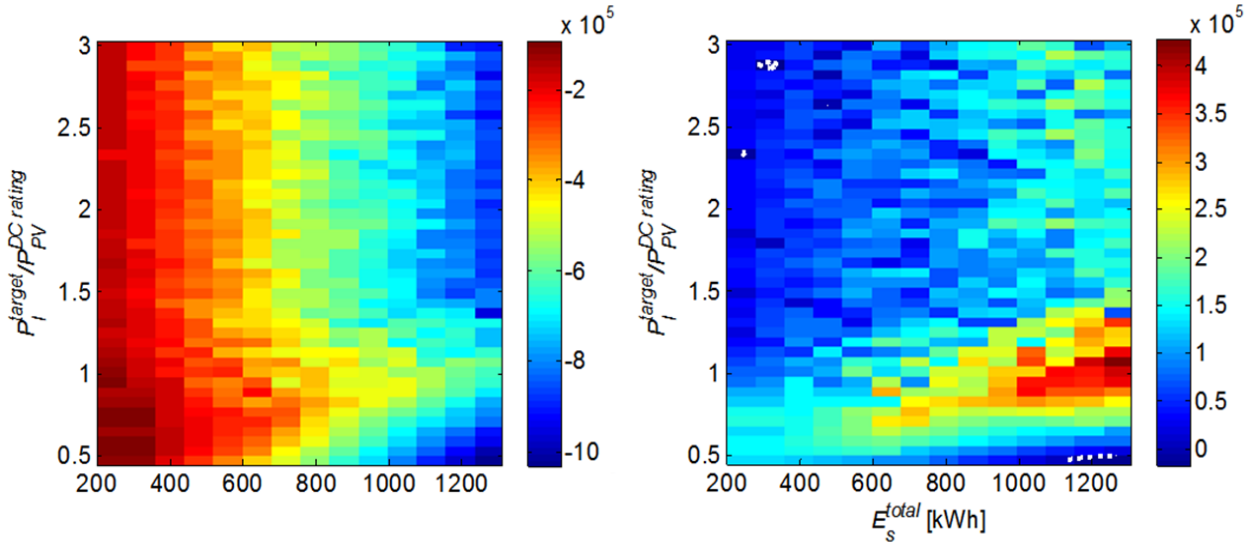

Figure 6 – The NPV of the battery array operated on the optimized dispatch schedule assuming an installed cost for storage of **(a)** \$1000/kWh and **(b)** \$200/kWh. The units of the color scale are \$USD and the dashed white line delineates the \$0 contour.

Fig. 6 illustrates the NPV of the battery array when operated under the optimized dispatch strategy assuming different costs for the storage. Fig. 6a shows the battery NPV assuming a cost \$1000/kWh, which is representative of the current (2011) market price for large scale, Lithium-ion battery arrays. At a price of \$1000/kW all battery sizes have a negative NPV indicating that Lithium-ion type batteries are not a financially viable technology in demand side applications if energy bill savings for the utility customer are the only value proposition considered in the valuation of the storage array. The results of Fig. 6a raise an interesting question: *What is the price at which Lithium-ion batteries become financially viable in demand side applications?* We estimated this price within our model framework by varying the capital costs in Eq. 6. Fig. 6b shows the NPV of the battery array at a cost of \$200/kWh, the maximum price at which the NPV > 0 for nearly all PV+ system designs modeled in this study. It is worth noting that the NPV of the battery array became greater than zero for a limited range of PV+ system parameters at a price as high as \$600/kWh.

Figure 7 shows the maximum NPV in USD as a function of battery energy storage capacity for three hypothetical storage costs \$600/kWh, \$400/kWh and \$200/kWh. At an installed cost of \$600/kWh only the battery capacities less than 400 kWh are profitable over the lifetime of the battery array and the marginal cost of storage is -123 \$/kWh. At installed costs of \$400/kWh and \$200/kWh all battery sizes are profitable and the marginal benefit of additional storage is 70 – 270 \$/kWh. In practice, when $E_s^{total} > E_l$ (or $P_l^{target} > sup\{P_l\}$) the slope of the lines in Fig. 7 becomes zero, because no additional demand charge savings can be realized.

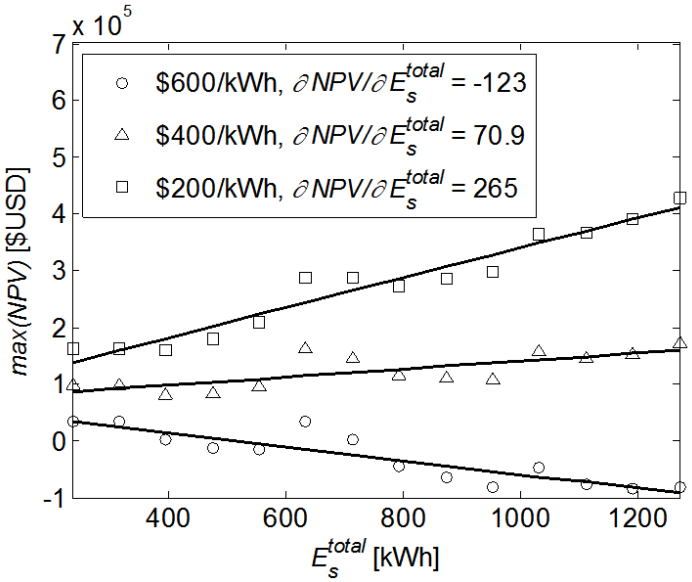

Figure 7 – The maximum NPV [\$USD] as a function of battery energy storage capacity assuming an installed cost for Lithium-ion batteries of **a)** \$600/kWh, \$400/kWh and \$200/kWh. For example, the data plotted as squares in this figure follow the maximum of the surface in Fig. 6b. The slope of the lines is the marginal cost of additional energy storage.

3.4 PV+ System Parameters at Maximum NPV

Fig. 8a shows that the peak load reduction target ratio ($P_l^{target}/P_p^{DC\ rating}$) and battery capacity ratio ($E_s^{total}/\langle E_l \rangle$; [11]) are linearly increasing functions of battery energy storage capacity. P_l^{target} is a relevant PV+ system parameter in the context of demand charge management because it is linearly related to the reduction in demand charges, however, in practice $E_s^{total}/\langle E_l \rangle$ is a more useful quantity for system design. Fig. 8b shows the financial value of the OPT dispatch schedule over the OFFON and RT dispatch schedules in terms of the difference in the NPV of the battery array (ΔNPV) as a function of the battery capacity ratio. ΔNPV in Fig. 8b can also be interpreted as value of the PV power output and load forecasts (see Section 4). Fig. 8b shows that the value of the forecasts increases linearly with $E_s^{total}/\langle E_l \rangle$ in the range \$150k - \$400k when compared to the ONOFF strategy. The trend in ΔNPV as a function of $E_s^{total}/\langle E_l \rangle$ is fairly weak for the OPT-RT data in Fig. 8b, and is better represented by the mean value of the data ($\langle \Delta NPV \rangle$ = \$51k) rather than a linear regression.

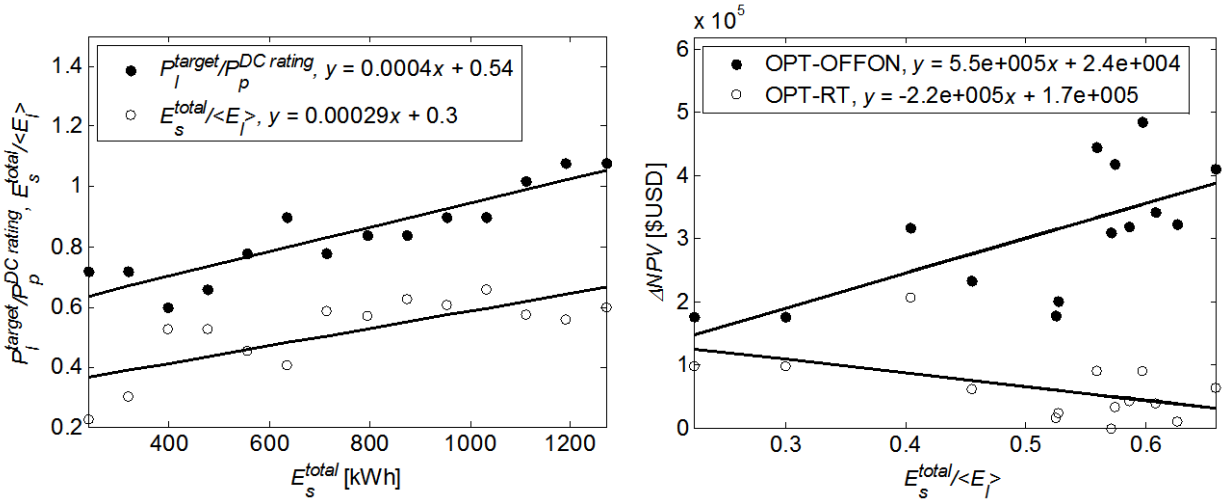

Figure 8 – **a)** PV+ system parameters as a function of the battery energy storage capacity (E_s^{total}) and **b)** the value of the optimized dispatch schedule (ΔNPV) as a function of battery capacity ratio ($E_s^{total}/<E_l>$) along the maximum of the surface in Figs. 6a and b. $<E_l>$ in Fig. 8a,b is the average daily energy consumption during the peak period (Fig. 1). The data in Fig. 8b correspond to the maximum of the surface plotted in Fig. 5.

4. Discussion

An important goal of this modeling effort was to demonstrate and quantify the value of applying PV power output and load forecasts to inform energy dispatch optimization in PV+ systems. The OFFON schedule maximizes price arbitrage in the time-of-use energy market, but its success as a demand charge management strategy relies on a strong temporal correlation between customer's actual peak load and the peak load period defined by the utility (Table 1). If the customer's actual peak load occurs outside the peak load period defined in the utility rate schedule the customer may incur high non-coincident demand charges (Table A.1). Because the peak load is typically variable over the on-peak market period, constant output from the battery over during the on-peak period market period is a robust yet suboptimal approach for demand charge minimization (e.g. Fig. 4a,d,g).

The effectiveness of the RT schedule primarily depends on whether the energy storage capacity of the battery exceeds the daily energy requirement of the customer's peak load ($<E_l>$). If the energy capacity of the battery is greater than the energy required to meet the customer's peak load, then energy stored in the battery can be dispatched in real-time and the entire peak load will be eliminated. If the battery capacity is less than the energy requirement of the load, the energy stored in the battery will be depleted before the peak load event (Fig. 4b,e,h), and the customer incurs high demand charges. The optimization algorithm developed in this paper improves on both the OFFON and RT strategies by using PV power output and load forecasts to overcome the disadvantages of both approaches. The optimal scheduling strategy targets demand charge management, because demand charges typically account for the largest portion of a utility customer's energy bill.

Fig. 5 quantifies the financial advantages of using PV power output and load forecasts to determine the optimal stored energy dispatch schedule in the PV+ system. We chose to present results as absolute USD values rather than percent values because, for an NPV that can be

positive or negative, absolute USD values provide readers with a more tangible quantity to interpret the relative value of different dispatch strategies. Fig. 5a shows that the largest financial gains from OPT strategy over the OFFON strategy occurred in the range in the range $E_s^{total} > 500$ kWh and $P_l^{target} / P_p^{DC\ rating} < 1.25$. Those gains were attributed to superior load following and reduced battery cycling characteristics of the optimized dispatch schedule. In the range $P_l^{target} / P_p^{DC\ rating} < 1.25$, the battery array lasts 8.2 year under the OFFON schedule compared to an approximately 10 – 16 year lifetime under the OPT schedule. The OPT dispatch schedule significantly increases the value of the battery array over the RT schedule for $E_s^{total} > 600$ kWh and $P_l^{target} / P_p^{DC\ rating} > 1.5$. These gains occur because the optimization strategy uses forecast information to distribute the energy stored in the battery over the duration of the peak load period, even when the energy capacity of the peak load exceeds the energy capacity of the battery array (Figs. 4h,i). In the range $P_l^{target} / P_p^{DC\ rating} < 1$ the performance of the OPT and RT dispatch strategies is similar because the energy capacity of the battery is greater than the energy capacity of the peak load so the amount of energy storage is sufficient to eliminate the peak load throughout the year, thus the dispatch schedules for both strategies are similar.

Noise in Figs. 5 and 6 is due to errors in the simulated PV power output and load forecasts relative to the actual PV output and load. Because forecasts are simulated using a Monte Carlo technique (Section 2.5), and a real-time dispatch strategy is used to respond to forecast errors between forecast updates (see Section 2.3) some random variability is expected across the range of simulations modeled in this study. The implication of the PV+ system real-time response to forecast errors is that, for erroneous forecasts that significantly and consistently under estimate the forecast net load (P_l-P_o), the OPT strategy reduces to the RT strategy as the forecast error becomes large. The small peak in Fig. 4i was found to be a common feature of the daily storage dispatch schedules produced by the optimization routine that occurred when the actual net load was underestimated by the forecasts. This finding is interesting because it suggests that there is an incentive to overestimate the magnitude of the net load in the forecast to improve performance of the battery. An alternative interpretation is that the financially optimal battery capacity will change based on the nature of errors contained in the PV output and load forecasts.

Generally the OPT schedule provides as much or greater value than the both the OFFON and RT schedules (in terms of the NPV of the battery array), but the optimization algorithm is only superior if reliable, accurate solar and load forecasts are available. Due to the structure of the demand charge tariffs, poor forecasts on only one day of the month could render the demand charge reduction of the OPT strategy inferior to OFFON. When no forecasts (or unreliable forecasts) are available, the PV+ operator must choose between the OFFON or RT schedule. Our results are significant in that context because, a typical PV+ owner/operator needs to purchase forecasts from a third party provider. The decision to purchase forecasts will depend on the priority of the PV+ system owner/operator and trends observed in a plot similar to Figs. 5 and 8b. Fig. 5 illustrates that the most financially attractive energy dispatch strategy for the PV+ system is a complex decision that depends on PV+ design parameters, electrical and performance characteristics of the battery array and utility energy prices.

Although the results of Fig. 5 and Fig. 8b are encouraging for the economics of solar and load forecasting in demand side energy storage applications Fig 6a indicates that at current (2011) market prices, no dispatch strategy performs well enough to make large scale Lithium-ion battery

energy storage a financially viable option if monthly energy bill savings are the only benefit associated with the operation of the energy storage. We employed our model to estimate the price at which Lithium-ion energy storage would become financially viable for the demand charge management application studied in this paper. Assuming a utility rate schedule similar to the SDGE AL-TOU battery array owners can expect to break even over the lifetime of the battery at an installed cost of $600/kWh for systems with batteries smaller than 400 kWh (Fig. 7). Larger capacity batteries (up to 1.25 MW) generate profits in the range $100k-200k (or $100-400 per kWh) at an installed cost of approximately $500-$400 per kWh (Fig. 7). This result is particularly relevant for the 2nd life battery industry, which holds promise for developing large scale Lithium-ion, battery energy storage systems from used EV batteries at a lower cost than new batteries. Perhaps the most interesting trend in Fig. 6 is that the PV+ system parameters which result in the most profitable design (in terms of the NPV of the battery array) change significantly depending on the market price of the battery. At the 2011 price of $1000/kWh all battery sizes return negative profits over the battery lifetime so it is logical that the most profitable battery size is the smallest size (Fig. 6a). If the market price for Lithium-ion batteries decreases sufficiently (Fig. 6b) nearly all battery capacities become profitable. In the price range of $200-$400 per kWh there is a marginal benefit associated with increasing storage capacity (until demand charges are eliminated) so that large capacity battery sizes have greater NPV than small capacity batteries, which is a desirable property in the sense of economies of scale (Fig. 7).

The similarity of the trends observed between the two variables plotted in Fig. 8a suggests that there is a strong correlation between the P_l^{target} and $<E_l>$. This observation is an indication that both $P_l^{target}/P_p^{DC\ rating}$ and $E_s^{total}/<E_l>$ are consistent and robust PV+ system parameters. The value of PV power output and load forecasts in demand side, energy bill management applications for large scale, Lithium-ion batteries is $51,000 ± $35,000 over the lifetime of the battery array, where the error is represented by one standard deviation of the OPT-RT data in Fig. 8b.

It is important for readers to realize that the results presented in this paper were based on site specific PV power output data and load profiles, and the SDGE AL-TOU rate schedule (SDGE, 2011). Some variability in Figs. 5 and 6 is expected on site to site basis. It has been noted that demand charges are typically higher in the state of California when compared to other regions in the United States (T. Pietsch, Personal communication, 2011). It is highly probable that a different rate schedule would produce different trends than those illustrated in Figs. 5 and 6. However, all of these differences are not related to any of the fundamental aspects of our model.

5. Conclusion

We developed a linear programming routine to optimize the energy storage dispatch schedule for a grid-connected, combined photovoltaic-battery storage system (PV+ system). The optimization strategy targets demand charge management through a targeted peak load reduction, and leverages PV power output and load forecasts to determine the best trajectory for the battery storage output power in order to minimize demand charges. We simulated a broad range of PV+ system designs and performed a cost analysis to compare the financial benefits of our optimized energy storage dispatch schedule with basic off-peak/on-peak charging/discharging and real-time dispatch strategies. The performance and value of the optimization method were quantified in terms of energy bill savings attainable over the lifetime

of the battery array. The net present value (NPV) of the battery array increased significantly (in the range $100k - $450k – or $220/kWh to $270/kWh – for some PV+ configurations) when energy storage was dispatched on the optimized schedule over the simple dispatch schedules that did not use forecast information. Lithium-ion batteries are not a financially viable storage technology in demand side, energy bill management applications at current (2011) market prices. We estimated that Lithium-ion batteries become profitable at an installed cost of about $450/kWh, which is about 45% of 2011 market prices. The value of PV power output and load forecasts for the application studied in this paper is $51,000 ± $35,000. This study underscores the need to develop tools and techniques for quantitative modeling and analysis to improve estimates of the economic value of energy storage and forecasting for both utility and demand side applications. We consider our method to be a simple yet feasible approach to that end, which is useful for energy storage manufacturers, financiers and other industry professionals seeking to quantify the value of their product and forecast investment returns.

Acknowledgements

The authors gratefully acknowledge Mike Chen (York University), Yu Ru (UC San Diego) and Joerg Wegener (UC San Diego) for their helpful comments and input. This project was motivated by discussion among the members of the EPRI subgroup during the 2011 Sustainability Problems Workshop hosted at the American Institute of Mathematics in Palo Alto, CA, USA. This research was supported by the United States Department of Energy High Penetration Solar Program under Award Number EE-0004680 and Panasonic Corporation.

References

1. United States Department of Energy (DOE), “States with Renewable Portfolio Standards,” <http://apps1.eere.energy.gov/states/maps/renewable_portfolio_states.cfm>, Accessed 11/19/2011.

2. J. Simitian, C. Kehoe, D. Steinberg, “California State Senate Bill No. 2 – Energy: renewable energy resources,” <http://www.leginfo.ca.gov/cgi-bin/postquery?bill_number=sbx1_2&sess=CUR&house=B&author=simitian>, Accessed 11/19/2011.

3. N. Skinner, “California State Assembly Bill 2514 – Energy storage systems,” <http://www.leginfo.ca.gov/pub/09-10/bill/asm/ab_2501-2550/ab_2514_bill_20100219_introduced.pdf>, Accessed 11/19/2011.

4. J. Eyer, G. Corey, Energy Storage for the Electricity Grid: Benefits and Market Potential Assessment Guide, Sandia National Laboratories, SAND2010-0815 (2010).

5. D. Rastler, Electric Energy Storage Technology Options: A White Paper Primer on Applications, Costs, and Benefits, EPRI, Palo Alto, CA, 2010. 1020676.

6. Andris Abele, Ethan Elkind, Jessica Intrator, Byron Washom, et al (University of California, Berkeley School of Law; University of California, Los Angeles; and

University of California, San Diego) 2011, ***2020 Strategic Analysis of Energy Storage in California***, California Energy Commission. Publication Number: CEC-500-2011-047.

7. K.C. Divya, J. Østergaard, Battery energy storage technology for power systems – An overview, Electric Power Systems Research 79 (2009) 511-520.

8. T-Y. Lee, N. Chen, Determination of optimal contract capacities and optimal sizes of battery energy storage systems for time-of-use rates industrial customers, IEEE Transactions on Energy Conversion 10(3) (1995) 562-568.

9. W-F. Su, C-E. Lin, S.J. Huang, Economic Analysis for demand-side hybrid photovoltaic and battery energy storage system, IEEE Transactions on Industry Applications 37(1) (2001) 171-177.

10. T.E. Hoff, R. Perez, R.M. Margolis, Maximizing the value of customer-sited PV systems using storage and controls, Solar Energy 81(7) (2007) 940-945.

11. T. Shimada, K. Kurokawa, Grid-connected photovoltaic systems with battery storages control based on insolation forecasting using weather forecast, Renewable Energy Proceedings (2006) 228-230.

12. Y. Ru, J. Kleissl, S. Martinez, Storage size determination for grid-connected photovoltaic systems, IEEE Transactions on Sustainable Energy (2012), arXiv:1109.4102v2 [math.OC].

13. M. Stadler, H. Aki, R. Firestone, J. Lai, C. Marnay, A. Siddiqui, Distributed Energy Resources On-site Optimization for Commercial Buildings with Electric and Thermal Storage Technologies, Lawrence Berkeley National Laboratory, LBNL-293E (2008).

14. M. Stadler, C. Marnay, A. Siddiqui, J. Lai, H. Aki, Integrated Building Energy Systems Design Considering Storage Technologies, Lawrence Berkeley National Laboratory (2009).

15. M. Stadler, C. Marnay, J. Lai, A. Siddiqui, T. Limpaitoon, T. Phan, O. Megel, J. Chang, N. DeForest, Storage Viability and Optimization Web Service, LBNL-4014E (2010).

16. San Diego Gas and Electric (SDGE), "Customer Rate Information – Schedule AL-TOU Secondary," <http://www2.sdge.com/tariff/com-elec/ALTOUSecondary.pdf>, Accessed 08/06/11.

17. M. Lave, J. Kleissl, E. Arias-Castro, High-frequency irradiance fluctuations and geographic smoothing, Solar Energy, doi: 10.1016/j.solener.2011.06.031.

18. P. Mathiesen, J. Kleissl, Evaluation of numerical weather prediction for intra-day solar forecasting in the continental United States, Solar Energy 85(5) (2011) 967-977.

Appendix A

Basic Service Fees	Usage [kW]	Fee [$/month]
	0-500	58.22
	>500	23.87
Demand Charges	**Time of Use**	**Fee [$/kW]**
	Non-coincident	15.20
	Summer On-peak	7.92
	Winter On-peak	5.31
Energy Charges	**Time of Use**	**Fee [$/kWh]**
	Summer On-peak	0.01388
	Summer Semi-peak	0.01091
	Summer Off-peak	0.01006
	Winter On-peak	0.01272
	Winter Semi-peak	0.01091
	Winter Off-peak	0.01006
Commodity Demand Charges	**Time of Use**	**Fee [$/kW]**
	Summer On-peak	4.90
	Winter On-peak	0.16
Commidity Energy Charges	**Time of Use**	**Fee [$/kWh]**
	Summer On-peak	0.08242
	Summer Semi-peak	0.06678
	Summer Off-peak	0.04926
	Winter On-peak	0.07993
	Winter Semi-peak	0.07349
	Winter Off-peak	0.05476
CA Department of Water Resources Bond Energy Charge	**Time of Use**	**Fee [$/kWh]**
	Non-coincident	0.00505

Table A.1 – The SDGE AL-TOU rate schedule (secondary) of default electricity rates for all non-residential customers whose monthly maximum demand equals, exceeds, or is expected to exceed 20 kW. The data in this table was current as of August 2011. Although electricity rates change every few months, the magnitude of the values shown in this table is representative of current TOU electricity rates for industrial customers in the SDGE territory. The TOU rate periods are defined in Table 1.